Characteristics of P and SH Waves in Shallow Seismic Reflection Surveys in the Putai Area

MING-TAR LU[1], CHIH-HSIN HU[2] and RUEY-CHYUAN SHIH[3]

ABSTRACT

A 100 meter long shallow seismic line was conducted at Putai to analyze the characteristics of P and SH waves. Vertical hammer-impact was the source for P waves and transverse hammer-impact was used to generate SH waves. From walkaway noise tests, the near-offset of P wave survey was chosen at 40 m and 10 m for SH wave survey to prevent interference from surface, direct and air waves. Since the velocities of SH waves in shallow structures are considerably low, the recording time was lengthened to cover interested targets. In the P and SH final stacked results, SH wave profiles have higher resolution than those of P waves. The shallowest events detected by SH waves were 10 m in depth, which is shallower than the 40 m ones of P waves, and consistent matching of reflectors indicates good correlation between P and SH wave profiles from 100 m to 230 m deep. Finally, the interval velocities of P and SH waves in the same layers were derived from processing stacking velocities, and then used to calculate Poisson's ratios for that layers. In this experiment, the calculated Poisson's ratios from 40 m to 250 m deep ranged from 0.49 to 0.46, which indicates wet and soft rocks in the shallow layers of this survey line.

(Key words: SH waves reflection, P waves reflection, Shallow seismic reflections)

1. INTRODUCTION

Seismic reflection surveys are commonly used in the petroleum industry and now have been newly developed for shallow engineering basement investigation. Stacked reflection profiles are directly used to interpret subsurface structures. In general, P wave methods are more widely used in seismic reflection surveys, since S wave methods involve some

---

[1] Taiwan Petroleum Exploration Division, Chinese Petroleum Corp., Miaoli, Taiwan, R.O.C.

[2] Formerly of the Institute of Seismology, National Chung Cheng University; presently of the HCK Geophysical Company, Taipei, Taiwan, R.O.C.

[3] Institute of Seismology, National Chung Cheng University, Minhsiung, Taiwan, R.O.C.

difficulties, such as energy attenuation and complicated field acquisition. S wave methods are more complicated than P wave ones; S waves have some characteristics not found in P waves. To better understand the petrophysics of the formations, it is necessary to integrate information from both P and S waves. In addition, the velocity of S waves is generally lower than that of P waves. If frequency contents of seismic signals for both P and S waves were the same, wavelengths of S waves would be shorter than those of P waves. That means S waves will have resolution higher than that of P waves. It is particularly obvious for shallow seismic reflections, since in shallower soft rocks P wave velocity can be many times that of S waves and the velocity of S waves in the hard bedrock is only about one half that P waves. Theoretically, S waves have higher resolution in shallower soft rocks; S wave reflection methods have a better chance of success in imaging shallow structures. In mapping shallow structures, since penetration is not too deep, the problem of energy attenuation of S waves can be easily overcome. Since there is no P to SV wave conversion in SH wave surveys, the use of SH waves instead of SV waves will be more suitable.

Shear wave sources are needed for SH wave surveys. In the field, transverse hammer-impact can be used to generate SH waves. At first, transverse hammer-impact from opposite directions are applied perpendicularly to the seismic line. Horizontal geophones are planted perpendicularly to the seismic line, too. Theoretically, impacts from opposite directions will generate polarity-reversed SH signals and P waves with the same polarity. Subtracting signals from the opposite directions, we will enhance SH wave and degrade P wave energy. Adding signals from opposite directions will then enhance the energy of P waves. For P and SH wave shallow seismic reflection surveys, near-offset geophones are easily interfered with by the massive noise of low velocity ground roll. Avoidance methods, by setting the receivers at large offset, are generally used to collect reflection signals that arrive before (or after) ground roll (Knapp and Steeples, 1986a, b; Hunter *et al*, 1984; Pullan and Hunter, 1985; and Wang, 1993). Additionally, the Common-Depth Point (CDP) techniques certainly help to increase S/N ratio (Knapp and Steeples, 1986a, b; Jongerius and Helbig, 1988). Though correlating P and SH wave signals for the same layer will probably be difficult for their different reflection coefficients, we think more detailed matching of reflectors between the two different profiles will help to realize their relationship. In this paper, we show results of P and SH wave shallow seismic reflection surveys conducted on the same line at Putai. Interval velocities of P and SH waves were evaluated from individual data processing and then used to calculate Poisson's ratio for that layer. The result was then used to describe the lithology of the formations.

2. P AND SH WAVE SHALLOW SEISMIC SURVEYS

In this paper, a seismic line about 100 meters long was laid out along a track of cropped rice field near Kuei-Lin elementary school at Putai (Figure 1) for experiments. The ground condition was wet and good for geophone coupling. During the experiment, a Geometrics ES 2401X 48-channel seismograph was used as the recorder. The analog signals were digitized into 15-bit digital data, and then stored in a hard disk. The selected low-cut filters have an 18 dB/octave roll off.

Vertical and transverse hammer-impacts were used to generate source signals for P and SH waves, respectively. One hundred Hz vertical geophones were used for P wave survey and twenty-eight Hz horizontal geophones were used for SH wave survey. Figure 2a illustrates the use of transverse hammer-impacts to generate SH waves. In the field, horizontal SH wave
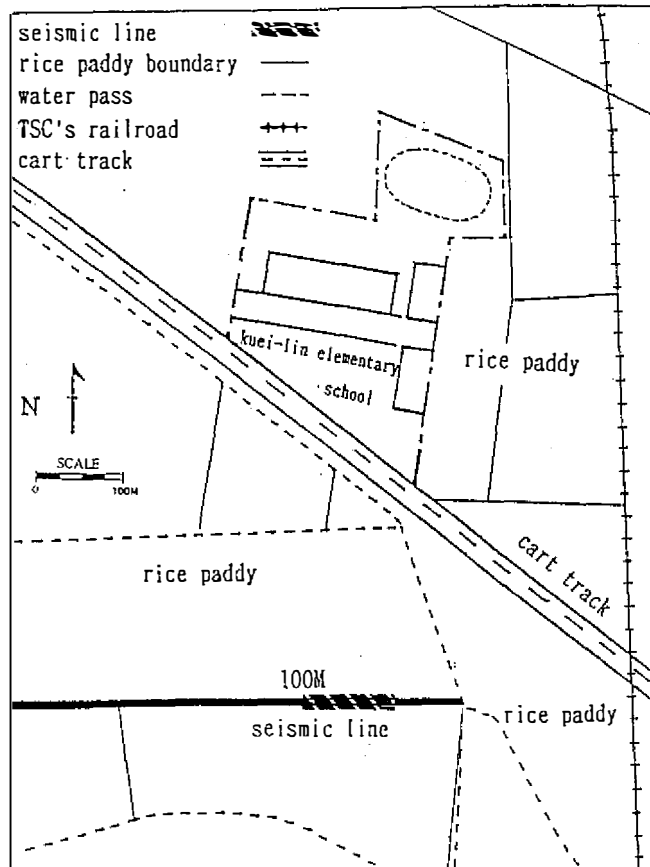
Fig. 1. Location map of the P and SH waves seismic survey line.

geophones were oriented perpendicularly to the survey line at each station. From the first transverse impact, signals of P waves were generated along with SH waves. The polarity of SH waves from this shot was marked as "+". Then a second transverse impact from the opposite direction was shot, and the generated SH wave was marked as "-". P waves were also generated in this shot, too. The two resulting seismograms contain SH waves of opposite polarity and the asymmetry of the shear properties in the zone of impact. P wave energy was also generated and recorded with individual shots, but the P wave amplitudes were of the same polarity on each of the seismograms. Theoretically, it is possible to constructively build up SH wave energy and cancel out P wave energy by subtracting the two recordings in data processing. Conversely, adding the two recordings would accentuate P wave energy and cancel SH wave energy (Figure 2b).

Recorded P and SH wave seismic data were processed on a SUN SPARC2 workstation with the software SIOSEIS. In the survey, the processing technology is primitive (Garotta, 1982), the individual component recordings are for the most part, processed independently. Processing parameters for each wave are often specified without considering their implications or contradictions with the parameters for another wave type.
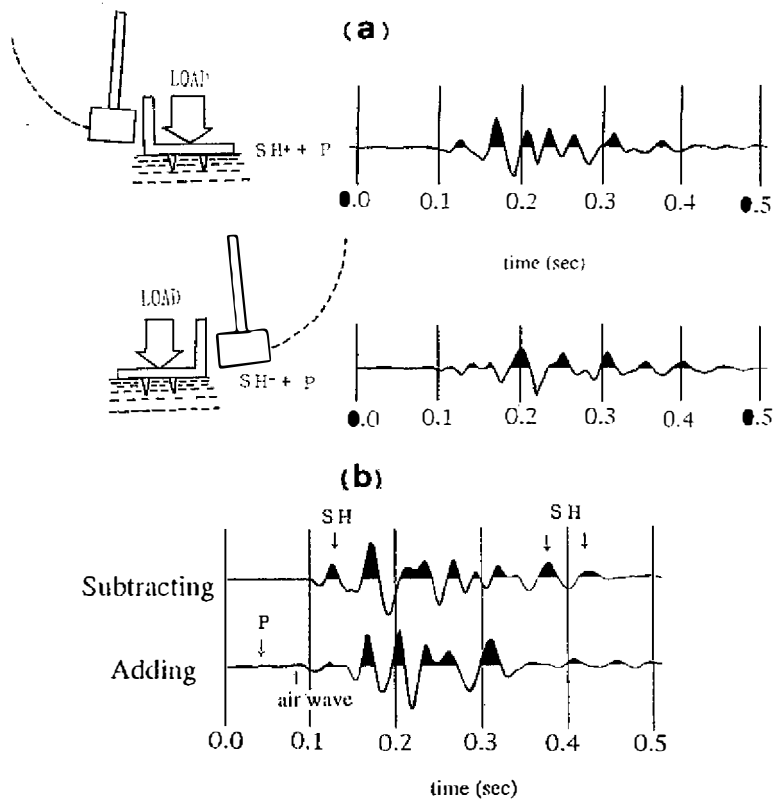
Fig. 2. (a) Transverse hammer impact and opposite direction impact generate reverse polarity SH waves. (b) SH wave energy built up after subtracting SH wave field recordings from opposite directions; contrarily, adding these two recordings accentuates P wave energy and cancels out SH wave energy.

The recorded high-amplitude refracted waves and unwanted noise were muted before processing. Bandpass filter was then used to eliminate low frequency ground roll (Rayleigh waves in P waves and Love waves in SH waves) and high frequency noises such as "air blast" originating from the source, wind noise and so on. Sorting the P and SH field records into CDP gathers can be accomplished using conventional gathering programs.

Usually, because of the difference in P and SH wave velocities, the magnitude of SH wave statics will be greater than P wave statics for the same location. In this paper, statics correction wasn't removed because: first, the stations are all at the same elevation; and second, SH wave statics are unreliable to estimate, because P wave to SH wave velocity ratio in shallow layers often spans a range. After a series of constant velocity analysis for the whole seismic section, normal moveout (NMO) corrections are applied to CDP gathers to move every trace to zero offset by using stacking velocities of P and SH waves. CDP stacked P and SH wave data are then displayed in time sections.

Assuming the shallow seismic reflections are horizontal and all offsets of the actual reflection events are zero, stacking velocity can be treated as root-mean-square velocity. Choosing corresponding stronger or characteristic reflections from both P and SH seismic

sections as formation intervals, we used Dix formula (Dix, 1955) to calculate the interval velocity. Interval velocity was then used to transfer time sections to depth profiles for both P and SH waves.

2.1 P Wave Experiment

The production of seismic profiles of P waves was preceded by walkaway noise tests. Source-to-receiver offsets on walkaway ranged from 2 to 192 m with receivers spaced at 2 m intervals. Figure 3 shows the record of walkaway noise test. Each record is the result of summing 8 blows of hammer and single high frequency 100 Hz geophone as receiver.

The P wave field parameters were determined by analyzing walkaway noise tests. Two of the shot records are shown in Figure 4. The production records were acquired with 0.5 msec sampling interval and the record length of 1000 msec to produce a 24-fold section. Seventy Hz analog low-cut and 250 Hz high-cut filters were applied in field. The dynamic range of the seismograph was wide enough to record the high amplitude of source generated noise and the high attenuation near surface at the seismic line. The near offset was 40 m with single receiver spaced at a 2 m station interval with a total of 49 shot points.
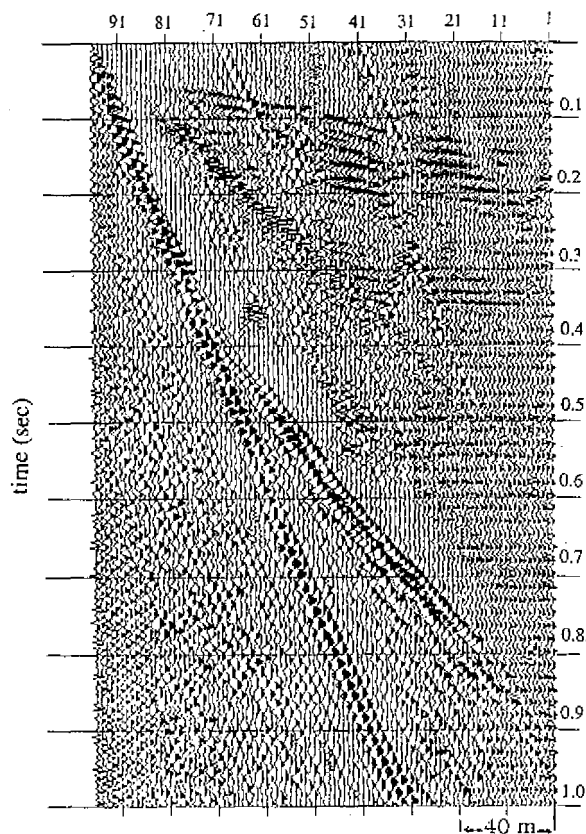
Fig. 3. P wave walkaway noise survey. Geophone was spaced at 2 m interval. Two 48-channel records were collected at 2 m and 98 m source offsets.

Figure 5 is the amplitude spectrum analysis of the 15th trace, from 0.25 to 0.35 second in P wave shot point 288. The dominant frequency of most reflection energy was 120 Hz; after a series of bandpass filter tests and velocity analysis, air waves in the range of 150 to 200 Hz high frequency, and band-pass filter 75 to 125 Hz were applied to the raw data. The determination of bandwidth and dominant frequency of the reflection signal allows ground roll energy to be effectively attenuated.
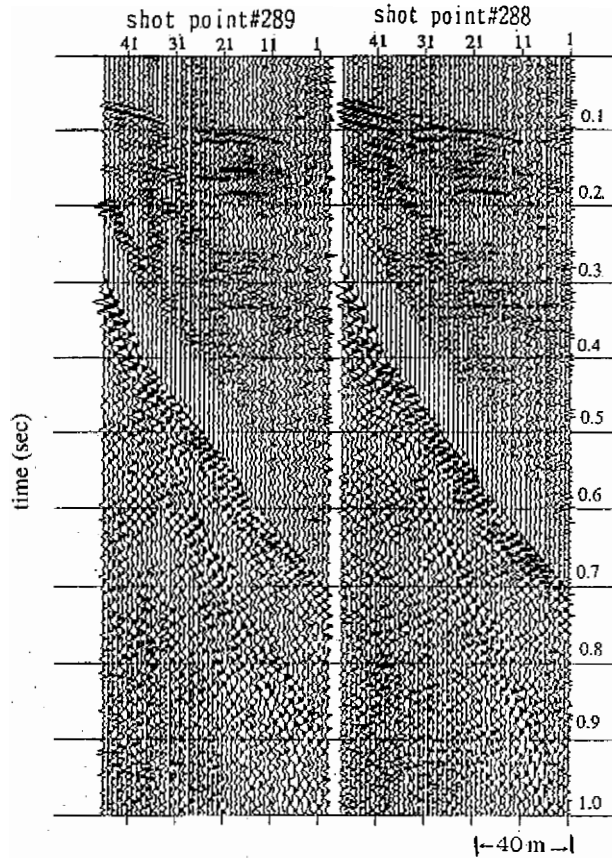
Fig. 4. P wave production raw record with 70 Hz low-cut and 250 Hz high-cut band-pass filtering, 40 m near offset, and 2 m station interval.
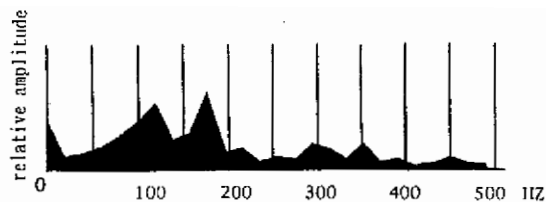
Fig. 5. Amplitude spectrum of the 15th trace, from 0.25-0.35 second in the P wave shot point 288 record.

Velocity (m/sec)
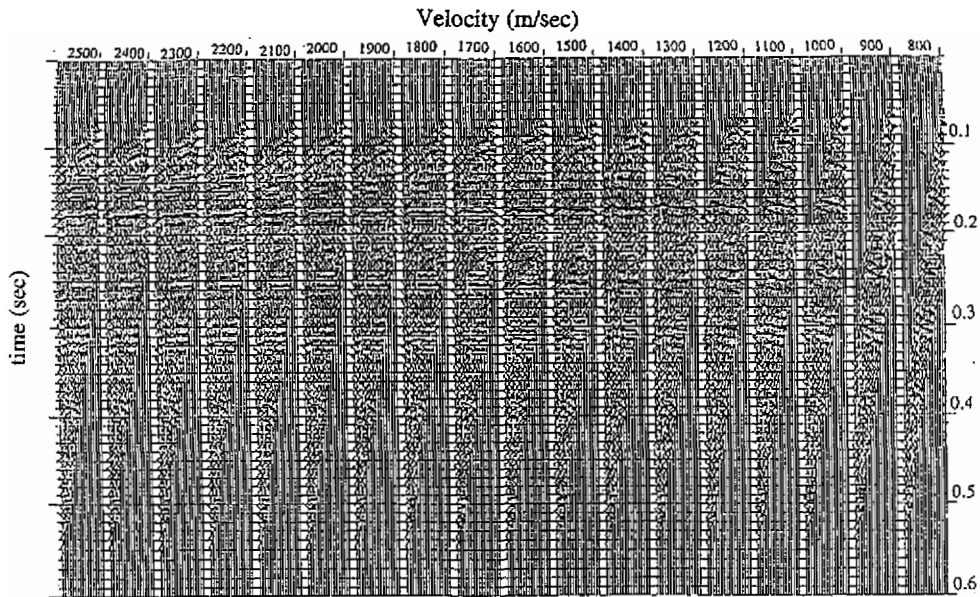
Fig. 6. P wave CDP gather constant velocity analysis.

Constant velocity analysis for the CDP gather (Figure 6) shows several reflection layers at 0.08, 0.17, 0.26 and 0.31 second. Applying optimum stacking velocities individually to NMO correction and CDP stack, we display P wave time section in Figure 7a. The calculated interval velocities were used to transfer the P wave time section to the depth plot. The shallowest layer P wave detected was of 40 m depth and the continuous reflections of 0.08, 0.17, 0.26 and 0.31 second correspond to depths of 40, 130, 230 and 300 m, respectively, in the depth profile of Figure 7b.

2.2 SH Wave Experiment

SH wave seismic line is located in the same position as the P wave experiment. Single 28 HZ horizontal geophones oriented perpendicularly to the profile were deployed at each station. Shear wave source was transverse hammer-impact applied in the direction perpendicular to the seismic line on the oblique pad. The obliquely angled pad excited obliquely polarized shear waves, while the horizontal component was recorded by the horizontal geophones. The source also excited P waves and ground roll, including both horizontally polarized Love waves and vertically polarized Rayleigh. Each record is summed of 8 blows SH impact to improve S/N ratio.

Figure 8 is the walkaway displays of SH waves with polarities marked "+" and "-". Source-to-receiver offset on walkaway tests ranged from 2 to 96 m with receivers spaced at 2 m intervals. Both P and SH wave walkaway sections are shown in Figure 9. In Figure 9, P wave reflections and air waves appear in front of the ground roll, at the upper right corner of the profile. As shown in Figure 9, SH wave reflections appear later than ground roll, and can be easily identified in the sections.

Figure 10 is the amplitude spectrum of the 46th trace, from 0.3 to 0.4 second in the SH shot record of Figure 9. The dominant frequency of most of the SH reflection energy is roughly from 10 to 30 Hz. After subtracting and adding the same SH walkaway shot point

(a)

W   50m   E   0.0

0.08 →   0.1

0.17 →   0.2

time (sec)

0.26 →   0.3

0.31→

0.4

0.5

(b)

W   50m   E   0.0

40 →

70 →   100

depth (meter)

130→

200

230→

300

400

500
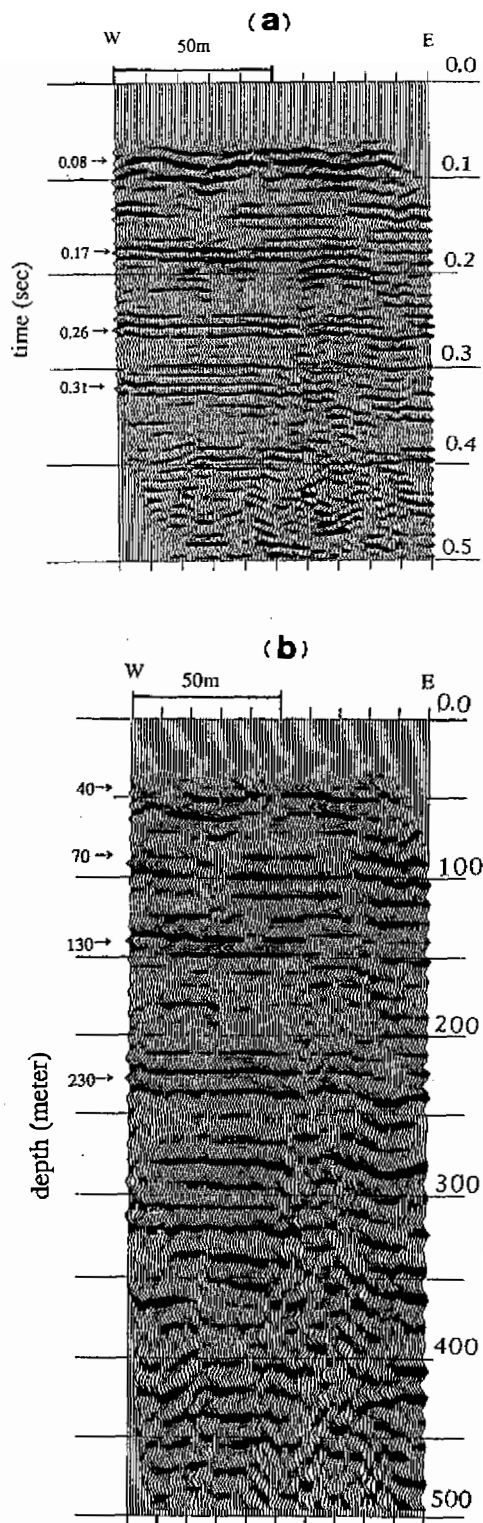
Fig. 7. (a) P wave CDP stacked section. (b) P wave shallow seismic depth profile.
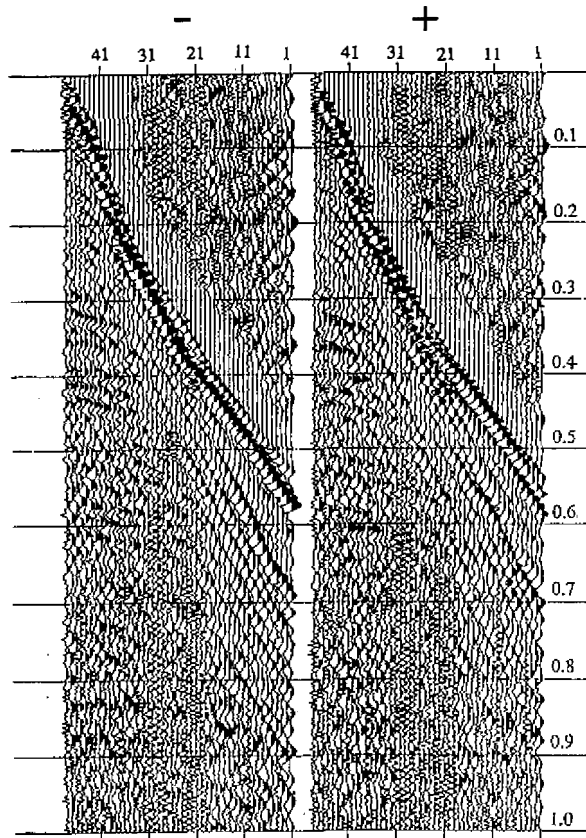
Fig. 8. SH wave walkaway noise tests displayed with "+" and "-" polarities.
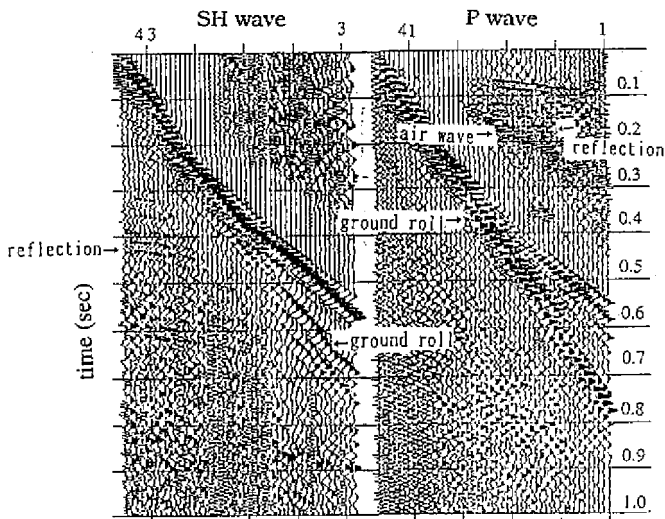
Fig. 9. P and SH wave walkaway noise tests sections, where reflection, ground roll and air wave are identified.

data with polarities "+" and "-" and applying a 15 to 30 Hz band pass filter, we show the results in Figure 11. In Figure 11, the subtracted reflections are more continuous and the S/N ratio is higher than that of the added ones. In addition, there are clearly reflections seen at 0.35, 0.55, 0.7 and 0.9 second.

The production line was acquired with no pre-filter, 10 m near-offset, 104 m far-offset, 0.5 msec sampling rate, and 1.5 second total recording time. Field data after subtracting and a 15 to 30 Hz bandpass filtering processes were then used to produce a 24 folds CDP section. Figure 12 shows one of the processed shot records. In Figure 12, the subtracting section shows reflections at near-offset, 0.55 to 0.9 sec, and the shorter near offset the better quality SH wave reflections were obtained. For adding sections, the P wave reflections usually appear in the right upper corner. More P wave reflection information was seen at the longer near-offset.
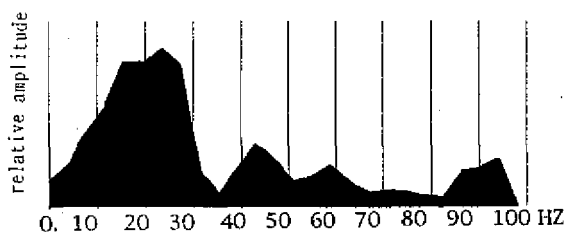
Fig. 10. The amplitude spectrum of the 46th trace, from the 0.3-0.4 second SH wave record.
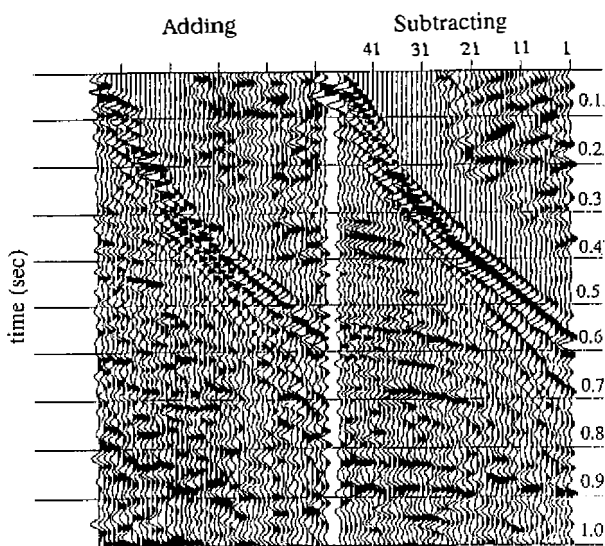
Fig. 11. After 15-30 Hz band-pass filtering, the "adding" and "subtracting" results of the same point SH walkaway data with "+" and "-" polarities.
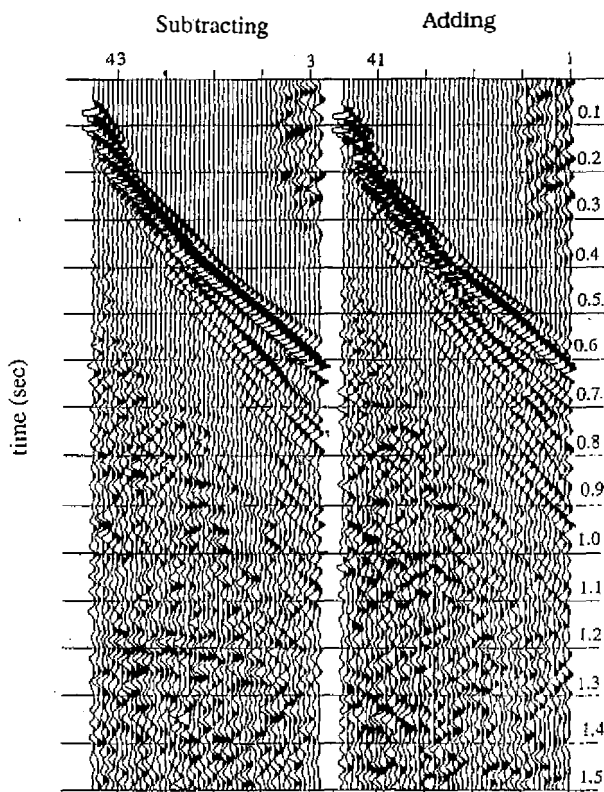
Fig. 12. Processed shot records from production line after subtracting and adding.

The data processing flow of SH waves is the same as that of P waves. Constant velocity analysis for CDP gather from 100 to 600 m/sec with increment of 50 m/sec are shown in Figure 13. In Figure 13, the corresponding stacking velocities for clear reflections at 0.2, 0.35, 0.55 and 0.75 sec are 150, 220, 250, 350 and 400 m/sec, respectively. After NMO and CDP stack, Figure 14a shows the SH wave time section. The quality of SH wave profile seems much better than that of P wave. Using the Dix formula to calculate interval velocity from stacking velocity and then transferring time section to depth profile, the results are shown in Figure 14b. As can be seen in Figure 14b, where SH wave section is clearer and more continuous than P wave.

Figure 15 shows the CDP stacked time profiles of both P and SH waves corresponding to the same depth. The shallowest layer of 0.15 second, equivalent to 10 m depth, is detected in the SH wave profile, where finer structure is delineated. Although the reflection impedance of P and SH waves may be different for the same layer, correlating major reflection events of 0.48, 0.55, and 0.7 sec on the P and SH wave sections, we may see confident correlation between these two sections. More detailed matching of reflectors in the intervals between the major reflection events are also seen. Figure 16 shows both P and SH wave depth profiles, where at the depths of 100 m, 135 m and 230 m, P and SH wave sections show clear and continuous reflections. However, at the record from 0 to 50 m, where P wave reflections are dim, the first reflection layer is around 40 m and SH waves are around 10 m in depth.
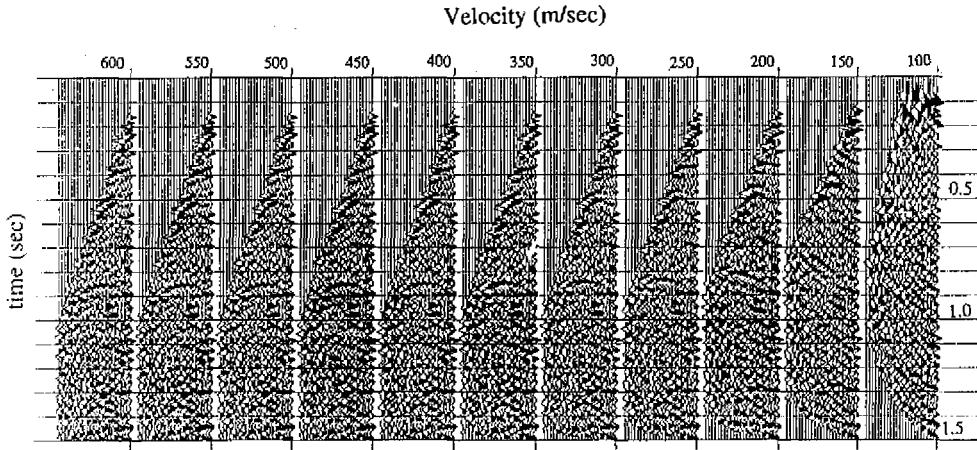
Fig. 13. SH wave CDP gather constant velocity analysis.
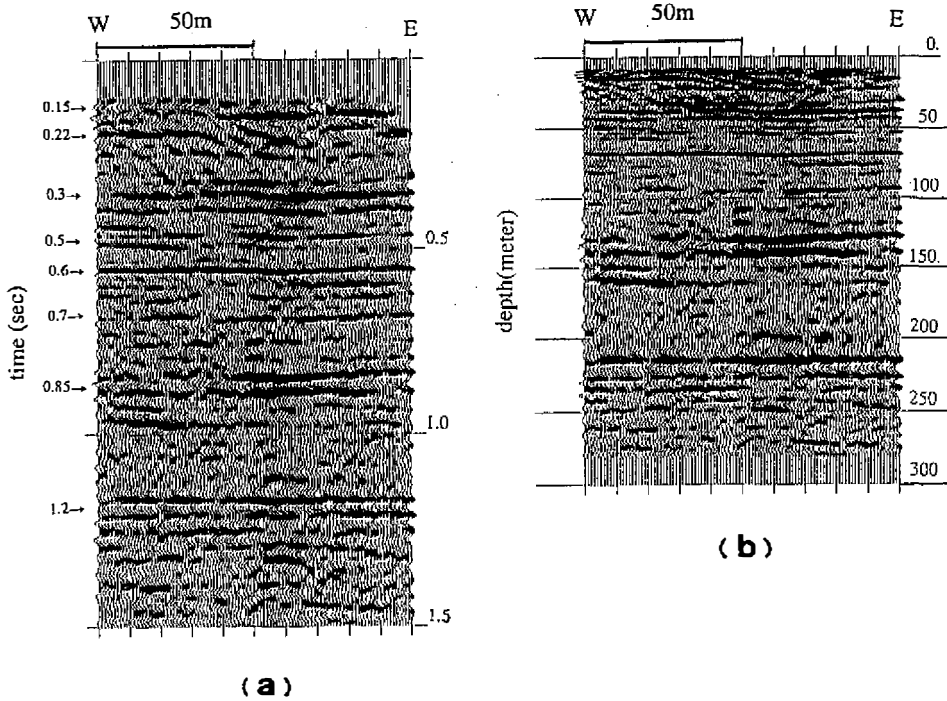
Fig. 14. (a) SH wave seismic time section. (b) SH wave seismic depth profile.
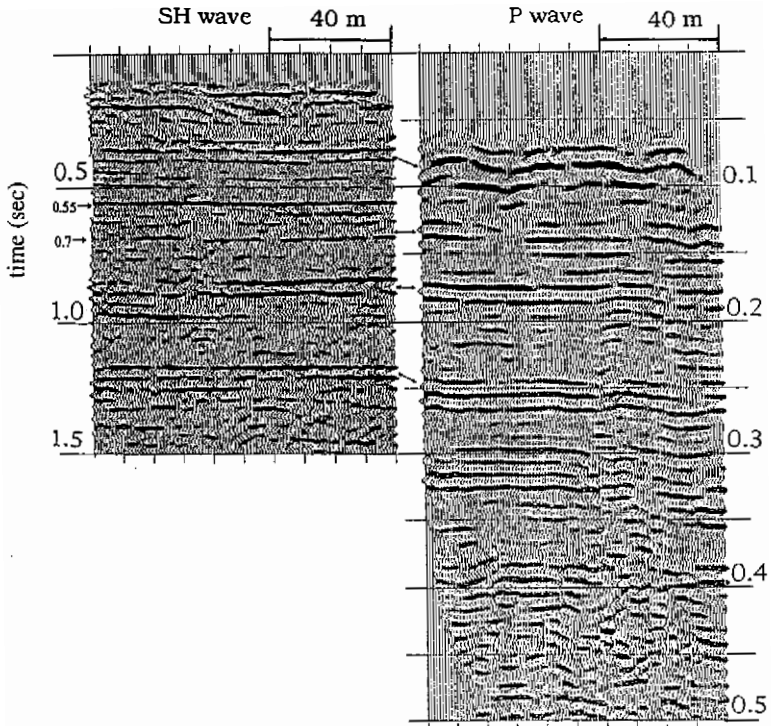
Fig. 15. P and SH wave time profiles corresponding to the same depth.
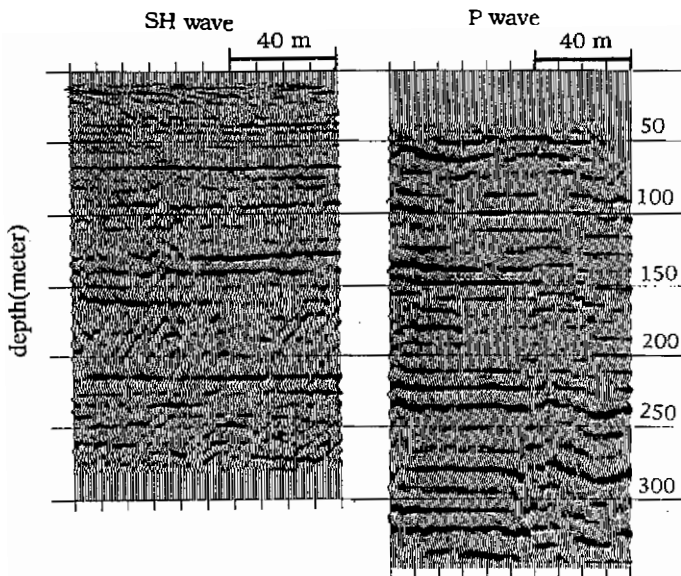
Fig. 16. P and SH wave depth profiles.

3. DISCUSSION AND CONCLUSIONS

Table 1 shows the stacking velocities and the calculated interval velocities for several layers of P and SH waves. Poissons'ratio can be calculated from surface to 250 m of depth for the corresponding P and SH interval velocities. The Poissons'ratio in the range of 0.49 to 0.46 means the formation is wet and soft (Hamilton, 1979).

In the walkaway noise tests of P and SH waves displayed in Figure 9, the first trace of about 0.55 sec to the 48th trace of 0.0 sec are characterized by slower velocity, high amplitude and low frequency. In the P wave section, Rayleigh waves and direct waves with velocity 160 m/sec appear. In the SH wave record, the mix of Love waves and direct waves with velocity 180 m/sec show. Love waves seem a little faster than Rayleigh waves, and can be detected earlier in the section. In the right upper corner of the P wave section, the higher frequency signals from the 48th trace at 0.0 sec to the first trace at 0.3 sec are air waves of velocity 350 m/sec. Because of the lower frequency (28 Hz) geophones used in SH wave survey, air waves are not detected in the SH wave section.

Table 1. Stacking and interval velocities of P and SH waves and their corresponding depths.

P wave

layer number	depth (m)	interval velocity (m/sec)	two-way travel time (sec)	stacking velocity (m/sec)
1		1100		
	40		0.08	1100
2		1939		
	130		0.17	1600
3		2127		
	230		0.26	1800
4		2819		
	300		0.31	2000
5		3419		
	600		0.5	2500

SH wave

layer number	depth (m)	interval velocity (m/sec)	two-way travel time (sec)	stacking velocity (m/sec)
1		150		
	10		0.2	150
2		287		
	40		0.35	220
3		295		
	70		0.55	250
4		406		
	110		0.75	300
5		525		
	230		1.2	400

Though better reflection signals appear in the longer offsets of the P wave shot records, in CDP stacking process, the large offset data were cut by using a 15% stretch ratio. In the SH wave section, the shorter offsets show better SH wave signals. In the SH wave survey, the nearest offset was chosen at 10 m and the recording time of SH waves was chosen as 1.5 sec, longer than the 1.0 sec for lower velocity P wave.

Comparing the P and SH wave profiles in Figure 15, SH wave reflections seem more continuous than P wave ones in the zone from 0.15 to 0.3 sec. In Figure 15, the discontinuous events in P waves are not a faulting effect; it was the interference of the noise that wasnt filtered in the data processing.

The depth studied in this paper is from surface to 300 m. In the P wave survey, the longer near-offset the more reflections will come in. Under the limited source energy condition, the 40 m near-offset is the optimum choice for this P wave survey. The shallowest layer detected is 40 m and there are more reflection events below 300 m of depth. In the SH wave survey, the shorter near-offset the higher quality signal will be detected. Since source impact at the zero near-offset position will create high amplitude noises to contaminate the record, 10 m near-offset is reasonable. The shallowest layer that can be identified is 10 m in the SH wave profile. Because of higher attenuation, SH waves can only penetrate to 250 m. Figure 16 shows that SH waves identify very shallow structures (smaller than 30 m. Miller et al., 1986) and also give higher resolution to reveal finer layers. P wave depicts structures deeper than 300 m. The combination of P and SH wave data provides extended coverage of depth, higher resolution of seismic quality and lithology information for whole seismic sections.

REFERENCES

Dix, G. H., 1955: Seismic velocities from surface measurements. *Geophysics*, **20**, 68-86.

Garotta, R., and D. Michon, 1982: Comparisons between P-SH-SV and converted waves, presented at the 52nd Ann. Internat. Mtg., Soc. Expl. Geophys., abs., and bio., 61-63.

Hamilton, E. L., 1979: Vp/Vs and Poissons ratios in marine sediments and rocks. *J. Acoust. Soc. Am.*, **66**, 1093-1101.

Hunter, J. A., S. E. Pullan, R. A. Burns, R. M. Gagne, and R. S. Good, 1984: Shallow seismic reflection mapping of the overburden-bedrock interface with the engineering seismograph-some simple techniques. *Geophysics*, **51**, 276-282.

Jongerius, p., and K. Helbig, 1988: Onshore high resolution seismic profiling applied to sedimentology. *Geophysics*, **52**, 1276-1283.

Knapp, R. W., and D. W. Steeples, 1986a: High-resolution common depth point seismic reflection profiling: instrumentation. *Geophysics*, **51**, 276-282.

Knapp, R. W., and D. W. Steeples, 1986b: High-resolution common depth point seismic reflection profiling: field acquisition parameter design. *Geophysics*, **51**, 283-294.

Miller, R. D., S. E. Pullan, J. S. Waldner, and F. P. Haeni, 1986: Field comparison of shallow seismic sources. *Geophysics*, **51**, 2067-2092.

Pullan, S. E., and J. A. Hunter, 1985: Seismic model studies of the overburden bedrock. *Geophysics*, **43**, 49-76.

Wang, C. Y., R. K. Yang, and D. T. Tsai, 1993: Shallow reflection seismic using firecrackers as the source II: field experiments. *TAO*, **2**, 163-186.